



## DESIGN AND OPTIMIZATION OF VOLTAGE MODE PWM CONTROL OF DC-DC BUCK CONVERTER WITH A PI-LEAD COMPENSATOR USING THE SIMULATED ANNEALING ALGORITHM

Kübra DOĞAN<sup>1\*</sup>, Bülent DAĞ<sup>2</sup>


<sup>1</sup>Gazi University, Faculty of Engineering, Department of Electrical and Electronic Engineering, 06500, Ankara, Türkiye


**Abstract:** This paper presents a method for improving the performance of DC-DC Buck Converter Systems using voltage mode Pulse Width Modulation (PWM) control. We explore the effectiveness of Proportional-Integral (PI) and Lead Compensator controllers in enhancing system stability, minimizing voltage fluctuations, and improving load response. The system is modeled through transfer functions, and the controllers' impacts are analyzed both individually and in tandem. A key contribution of this work is the optimization of the PI-Lead Compensator parameters utilizing the Simulated Annealing Algorithm, which is fine-tuned to improve phase margin, gain crossover frequency, and steady state error. These parameters are critical for optimizing the system's output performance. Through MATLAB simulations, we demonstrate the iterative process of parameter optimization and validate the algorithm's efficacy in managing the DC-DC Buck Converter. The results highlight the enhanced performance achieved with the optimized parameters, providing a viable solution for effective control of DC-DC Buck Converter Systems.

**Keywords:** DC-DC Buck Converter, Voltage Mode PWM Control, PI-Lead Compensator, Simulated Annealing Algorithm

\*Corresponding author: Gazi University, Faculty of Engineering, Department of Electrical and Electronic Engineering, 06500, Ankara, Türkiye

E mail: kubradogan@aselsan.com.tr (K. DOĞAN)

Kübra DOĞAN  <https://orcid.org/0009-0006-9099-9058>

Bülent DAĞ  <https://orcid.org/0000-0002-1404-232X>

Received: October 27, 2023

Accepted: November 27, 2023

Published: January 15, 2024

**Cite as:** Doğan K, Dağ B. 2024. Design and optimization of voltage mode pwm control of dc-dc buck converter with a pi-lead compensator using the simulated annealing algorithm. BSJ Eng Sci, 7(1): 72-88.

### 1. Introduction

In contemporary times, energy efficiency and power conversion are fundamental requirements in modern electronic systems. DC-DC converters encompass numerous topologies widely employed for power conversion purposes. These topologies are significant in achieving energy efficiency and power conversion in electronic systems. Power converter topologies transform a source voltage into a different voltage level and typically exhibit circuit structures characterized by high efficiency, low noise, and fast response time (Umanand, 2009; Rashid, 2010; Volkov, 2015; Rashid, 2017)

Generally, the operating principles of DC-DC Converters can be analyzed within two major categories: DC-DC linear and DC-DC switched-mode converters. DC-DC linear converters utilize the principle of linear regulation to control the input voltage and maintain the output voltage at a specific level, operating as active power-controlled converters. Energy flow is often controlled using a transistor or an electronic switch. The advantages of DC-DC linear converters include low power consumption, low cost, simple design requirements, and precise voltage regulation to maintain the desired output voltage. The disadvantage of DC-DC linear converters is

typically their low efficiency. Therefore, DC-DC linear converters are typically used to regulate the input voltage to a constant output voltage in low-power applications. On the other hand, DC-DC switched-mode converters or switched-mode power supplies are commonly preferred in applications requiring high power or where energy efficiency is critical. In these converters, switches such as transistors, MOSFETs, IGBTs, etc. control the energy flow. DC-DC switched-mode converters offer numerous advantages. In the presence of voltage oscillations, unbalanced loads, and similar situations, it provides high efficiency by utilizing feedback control mechanisms to maintain the desired output voltage. By rapidly switching the switches, energy losses are minimized, resulting in more effective energy conversion. These converters can be utilized in various power levels, from low-power to high-power applications. However, DC-DC switched-mode converters also have some disadvantages. The design, control, and implementation of DC-DC switched-mode converters can be complex. The correct timing and control of the switches may require additional electronic components or control algorithms (Middlebrook and Slobodan, 1976; Bose, 2002; Ogata, 2010; Rashid, 2010; Basso, 2014; Kazimierczuk, 2015; Erickson and Maksimović, 2020;



Bose, 2020).

Switched-Mode Power Supplies (SMPS) encompass different configurations, such as isolated and non-isolated configurations. Isolated converters basically include flyback converter, forward converter, and full-bridge converter. On the other hand, non-isolated converters consist mainly of Buck Converter, Boost Converter, and Buck-Boost Converter. In this paper, the Buck Converter, which is commonly used among non-isolated DC-DC SMPS, has been discussed. The DC-DC Buck Converter is an electronic circuit that efficiently steps down the energy from power sources to produce the desired output voltage at a lower voltage level (Moorthi, 2005; Ogata, 2010; Rashid, 2010; Rashid, 2017; Suntio and Messo, 2019).

In DC-DC Buck Converters, the output voltage must reach the desired value quickly and accurately, directly affecting the converter's performance. However, voltage fluctuations and load changes can cause the output voltage to deviate below or above the desired value. Therefore, various control methods are employed to optimize the converter's performance. Pulse-Width Modulation (PWM) and Frequency Modulation (FM) are the two main techniques used to control the output voltage of the DC-DC Buck Converter. In the PWM method, the converter's switches are turned on and off at a specific frequency, creating pulses. This method includes control methods such as voltage mode and current mode control. In the FM method, the switching frequency is continuously changed to achieve a constant pulse. Both of these control techniques are used to keep and control the output voltage of the DC-DC Buck Converter at the desired level. In this paper, the voltage mode PWM control method has been employed to adjust the output voltage of the DC-DC Buck Converter to the desired level (Middlebrook and Slobodan, 1976; Mohan and Tore, 2003; Umanand, 2009; Basso, 2014; Suntio and Messo, 2019; de 2021).

The voltage mode PWM control method is a widely used method in DC-DC converters to precisely adjust the desired output voltage by changing the pulse width of the switching signal. The output voltage is continuously measured and compared to the reference value. As a result of this comparison, an error signal is obtained, which is then fed back into the converter's switching circuit. The switching frequency and amplitude are adjusted based on the characteristics of this error signal. As a result, the output voltage is maintained at the desired level. The voltage mode PWM control method offers advantages such as superior voltage regulation, high precision, low output impedance, and stable operation. Additionally, its ability to respond rapidly to changes in output voltage makes it applicable to various applications (Mohan and Tore, 2003; Moorthi, 2005; Umanand, 2009; Basso, 2014; Kazimierczuk, 2015; Rashid, 2017; de Azpeitia, 2021).

In voltage mode PWM control, various control methods are employed to precisely adjust the pulse width of the

switching signal to achieve the desired output voltage: Proportional-Integral-Derivative (PID) Controller, Lead Compensator, Lag Compensator, Lag-Lead Compensator, etc. The PID Controller provides a fast response and appropriate settling times within the feedback loop. The P term rapidly adjusts the output voltage; the I term corrects steady-state errors; the D term enhances the system response speed. Similarly, compensator methods are control strategies that enable a DC-DC Converter to respond quickly to various load and input voltage conditions and ensure stability in the output voltage. This control system continuously measures the output voltage through a feedback loop and performs corrective actions. The Lead Compensator, one of the most commonly used, is typically employed to increase the Phase Margin (PM) value and speed up the system response. However, it might decrease the system's Gain Margin (GM) value. Conversely, the Lag Compensator is predominantly used to boost the Gain Margin value and diminish Steady-State Errors (SSE). However, it can reduce the Phase Margin value. Given the necessity to strike a balance between Phase and Gain Margin values, the Lag and Lead Compensator methods are usually used in conjunction. The term "Phase Margin" mentioned here indicates how close the phase of a control system is to -180 degrees at the frequency where the system's gain crosses 0 dB in the Bode Plot of the frequency response. In other words, it shows how close the phase is to -180 degrees when the system's frequency is at 0 dB. Systems with higher Phase Margins are typically more resilient to phase disturbances caused by external factors. Ideally, the Phase Margin should be between 45 to 60 degrees. On the other hand, "Gain Margin" indicates how close the magnitude of the system is to 0 dB at the frequency where the system's phase is at -180 degrees. In other words, it shows how close the magnitude is to 0 dB when the phase is at -180 degrees. A system with higher Gain Margin is generally more robust against magnitude disturbances caused by external factors. Ideally, the Gain Margin should be at least 6 to 10 dB (Franklin et al., 2002; Moorthi, 2005; Pressman, 2009; Ogata, 2010; Bishop and Dorf, 2011; Rashid, 2017; Nise, 2020; de 2021).

Various control methods can be combined to achieve desired performance objectives in voltage mode PWM control for DC-DC Converters. There are numerous studies related to combined control methods. In (Feng et al., 2023), a temperature control process was carried out using a PID Controller in conjunction with the PWM method (Qu et al., 2023), Fuzzy Logic and PWM methods were used together, and it was reported that this structure provided better performance than a PID controller. Amaral and Antonio (2022a), presented PWM signal generation in connection with a Type-II Controller for a non-isolated DC-DC Buck Converter. In Zebet et al. (2021), Adaptive-PI (A-PI) and Adaptive-Sliding Mode Controller (A-SMC) have been used together. Garg et al. (2015), PI Controller and Lead Compensator control

methods have been used together to regulate the output voltage based on frequency domain characteristics.

As mentioned in the previous paragraph, various advantages can be obtained when control methods are used together. Among these advantages are reaching the desired output voltage value quickly and accurately, reducing fluctuations in the output voltage, increasing stability, responding rapidly to load changes, and maintaining the output voltage at the desired level. Furthermore, the option to try different combinations of control methods provides design flexibility. However, combining multiple control methods can also lead to a complex design process that requires precise analysis and careful calibration to prevent potential instability (Franklin et al., 2002; Ogata, 2010; Rashid, 2017; Nise, 2020).

This paper aims to provide an effective and optimal approach for achieving the desired performance in DC-DC Buck Converters using voltage mode PWM control by combining PI Controller and Lead Compensator methods. This combination reduces output voltage fluctuations and enhances stability by enabling quick and precise attainment of the desired output voltage. The PI Controller measures the output voltage through a feedback loop and calculates the errors that need to be corrected. On the other hand, the Lead Compensator allows faster dynamic response by reaching the desired output voltage more quickly. During this integrated design process, obtaining the most appropriate settings to address instability issues and meet the desired performance goals effectively is crucial. In this integrated design process, obtaining the most suitable settings is crucial to address instability issues and effectively meet the desired performance goals. At this stage, utilizing heuristic algorithms, which is the most significant contribution of this publication, allows practical solutions and optimal adjustments for the complex design process (Franklin et al., 2002; Pressman, 2009; Bishop and Dorf 2011; Eiben and James, 2015; Erickson and Maksimović, 2020).

Heuristic algorithms are problem-solving algorithms that aim to obtain good results close to the desired values by evaluating various alternatives within a reasonable time without placing too much emphasis on the provability of the result. They do not guarantee that the best result will always be obtained because they are approximation methods. However, they generally reach a solution path that is quick, easy, and closest to the best possible outcome (Glover and Gary, 2006; Yang, 2020).

Different heuristic algorithms can be used in the controller design: Genetic Algorithm, Particle Swarm Optimization, Simulated Annealing, etc. These methods provide effective options for exploring and improving design parameters. It is important to note that each algorithm offers a different approach to optimize the complex design process and enhance performance by meeting design criteria. These algorithms have various advantages and disadvantages. Therefore, selecting a

suitable algorithm based on design requirements and priorities is crucial (Glover and Gary, 2006; Eiben and James 2015; Yang, 2020).

The most significant contribution of this paper is the utilization of the Simulated Annealing (SA) Algorithm to optimize the complex design process and enhance the performance of DC-DC Buck Converters. The SA Algorithm has facilitated the design process by optimizing the parameters of the PI-Lead Compensator used in the voltage mode PWM control method for fast and optimum adjustment of the desired output voltage in the DC-DC Buck Converter system.

The SA Algorithm is a search algorithm that seeks the best solution while navigating the potential solution space when determining an objective function that needs to be optimized. As the algorithm randomly traverses the solution space, it keeps the current solution open to changes and improvements for an acceptable period. In this way, by searching across a broad area of design parameters, it explores potential solutions for better performance (Glover and Gary, 2006; Chibante, 2010).

The SA Algorithm can offer numerous advantages when used in compensator design. First, its ability to explore design parameters by searching within an ample solution space can improve the output performance of the DC-DC Buck Converter. Another advantage of the algorithm is its flexible structure, which can be adapted to different design objectives. Furthermore, taking random steps in the complex design space can resist challenges such as balancing problems and adjusting difficulties while approaching the global optimum. However, using the SA Algorithm in compensator design can also entail certain disadvantages. For instance, in scenarios with many parameters to optimize, computational time and resource requirements may increase (Glover and Gary, 2006; Yang, 2020).

In the design of the DC-DC Buck Converter, for the SA Algorithm to function efficiently, it is essential to define the objective functions correctly. The need for a precise mathematical formula for the DC-DC Converters has been a complicating factor in their design. Therefore, in these converters, correct analysis and modeling of the system are essential to achieve the desired performance. This analysis can be conducted using various mathematical modeling methods, such as state-space models, transfer functions, small-signal linearization and compact models. These methods play a significant role in the design and optimization process of the converters (Bose, 2002; Mohan and Tore, 2003; Chibante, 2010; Rashid, 2010; Erickson and Maksimović, 2020).

Another contribution of this paper is using the duty-cycle-to-output-voltage transfer function method, obtained with the state-space averaging technique, for the mathematical model of DC-DC Buck converters. Considering the circuit's dynamics, this technique takes long-term averages at the circuit's operating frequency. Thus, the obtained transfer function describes the relationship between the circuit's duty cycle and the

output voltage. As a result, it becomes possible to obtain results that are close to the system responses. Due to its ease of use, the transfer function method is preferred over other mathematical modeling techniques, such as state-space representation, small-signal linearization, and compact models. It provides significant ease in the design and optimization process (Franklin et al., 2002; Pressman, 2009; Corradini, 2015).

Another significant contribution of this article is considering the parasitic components while deriving the transfer function of the DC-DC Buck Converter circuit. The goal is to obtain a more detailed mathematical model than the standard DC-DC Buck Converter transfer function to achieve accurate results that closely resemble the system responses (Franklin et al., 2002).

When the detailed extracted transfer function of the DC-DC Buck Converter system is analyzed for frequency and step response reactions, it is often observed that the PM value is low, and the Gain Crossover Frequency (GCF) or bandwidth remains constant at low frequencies. Additionally, the SSE value in an unregulated Buck Converter is generally very high. So, without a feedback loop or control algorithm, there can be a significant overshoot and some error in the output voltage. Therefore, designing the most suitable controller is of great importance to achieve the desired performance characteristics of the system. Thanks to the SA Algorithm, the error margin is almost reduced to zero, aiming to achieve a fast and accessible design (Mohan and Tore, 2003; Ogata, 2010; Rashid, 2010; Garg et al., 2015; Erickson and Maksimović, 2020).

The most significant contribution of this paper is the utilization of the Simulated Annealing Algorithm to optimize the PI-Lead Compensator parameters in a DC-DC Buck Converter system based on the accurate and detailed analysis of the mathematical model. In this optimization process, the PI-Lead Compensator parameters are optimized to bring critical values such as PM, GCF, and SSE to the desired levels, aiming to improve the system's performance accordingly.

The remainder of this paper is organized as follows. Section 0 presents a mathematical model of the Buck Converter system. This model incorporates parasitic components for realistic system response. The technique of state-space averaging is employed to derive the duty-cycle-to-output-voltage transfer function. Section 0 lays out the detailed design of a PI-Lead Compensator added to the Buck Converter system. This state facilitates Closed-Loop voltage mode PWM Control. In Section 0, the process of tuning the parameters of the PI-Lead Compensator using the Simulated Annealing Heuristic Optimization Algorithm is explicated. This process aims to improve values of the Buck Converter in both the frequency and time domain (PM, GCF or Bandwidth, the corner frequency of the PI Compensator, and SSE). Additionally, the open-source project, which enabled the optimization of PI-Lead Compensator parameters and performance analysis for DC-DC Buck Converters using

the SA Algorithm and developed in MATLAB, has been added as Buck-Converter-PI-Lead-Compensator-SA (2022). Section 5 features the performance outcomes obtained by adapting the optimized PI-Lead Compensator parameters to the DC-DC Buck Converter system using the Simulated Annealing Algorithm. Following these sections, the conclusion and discussion parts are presented.

The introduction should briefly place the study in a broad context and highlight why it is important. It should define the purpose of the work and its significance. The current state of the research field should be carefully reviewed and key publications cited. Please highlight controversial and diverging hypotheses when necessary. Finally, briefly mention the main aim of the work and highlight the principal conclusions. As far as possible, please keep the introduction comprehensible to scientists outside your particular field of research.

## **2. Materials and Methods**

### **2.1. Transfer Function Mathematics Model of Dc-Dc Buck Converter**

The transfer function of a DC-DC Buck Converter circuit is a function that expresses the mathematical relationship between the input and output. This function can be derived for both ideal and non-ideal cases (Ogata, 2010; Rashid, 2010).

When the DC-DC Buck Converter circuit is to be analyzed in the ideal case, the circuit's transfer function is derived as if there is a precise mathematical relationship between the input and output, disregarding all energy losses, parasitic effects, and delays. In this scenario, the converter is considered completely efficient and a perfect device that accomplishes the desired conversion. However, in practice, achieving such an ideal converter is not possible due to the limitations of real-world components. Nevertheless, ideal transfer functions are helpful for analysis and understanding fundamental principles (Ogata, 2010; Rashid, 2010; Garg et al., 2015; Erickson and Maksimović, 2020).

For non-ideal cases, the transfer functions of converters are derived by considering parasitic elements, energy losses, and other real-world effects. These transfer functions provide a more accurate representation of the behavior of real-world converters. Due to the limitations of real components, non-ideal transfer functions can be more complex, and mathematical calculations may be more challenging (Ogata, 2010; Rashid, 2010; Garg et al., 2015; Erickson and Maksimović, 2020).

The functioning modes of DC-DC Buck Converters significantly impact the transfer function's derivation and the control strategy's development. Generally, these converters function in two primary modes: Continuous Conduction Mode (CCM) and Discontinuous Conduction Mode (DCM) (Ogata, 2010; Rashid, 2010; Garg et al., 2015; Erickson and Maksimović, 2020).

The inductor current never falls to zero in the CCM. This mode is typically seen when the load is high. CCM is more



straightforward from a mathematical modeling perspective, assuming the continuity of the inductor current. On the other hand, in the DCM, the inductor current drops to zero for specific periods. This situation typically occurs when the load is lower. DCM is more complex from a mathematical modeling perspective as it needs to consider the discontinuity of the inductor current. Both operating modes can significantly affect the derivation of the transfer function and the overall performance and stability of the converter. Therefore, a detailed understanding of these operating modes is crucial for creating an effective control strategy (Ogata, 2010; Rashid, 2010; Garg et al., 2015; Erickson and

Maksimović, 2020; Nalepa, Karol and Błazej, 2020; Yang et al., 2020; Surya and Sheldon, 2021; Surya, Mohan and Sheldon, 2021; Wang, Bingwen and Hongdong, 2021; Amaral and Antonio, 2022b).

The schematic representation of a non-ideal DC-DC Buck Converter, functioning in CCM and considering its parasitic impedances, is illustrated in figure 1. The circuit includes a single switch ( $S$ ) along with its parasitic resistance ( $r_{sw}$ ), a single diode ( $D_d$ ) and its forward resistance ( $r_d$ ), an inductor ( $L$ ) and its ESR parasitic resistance ( $r_L$ ), a capacitor and its ESR parasitic resistance ( $r_c$ ), and finally, a load resistor ( $R$ ) (Ogata, 2010; Rashid, 2010; Erickson and Maksimović, 2020).

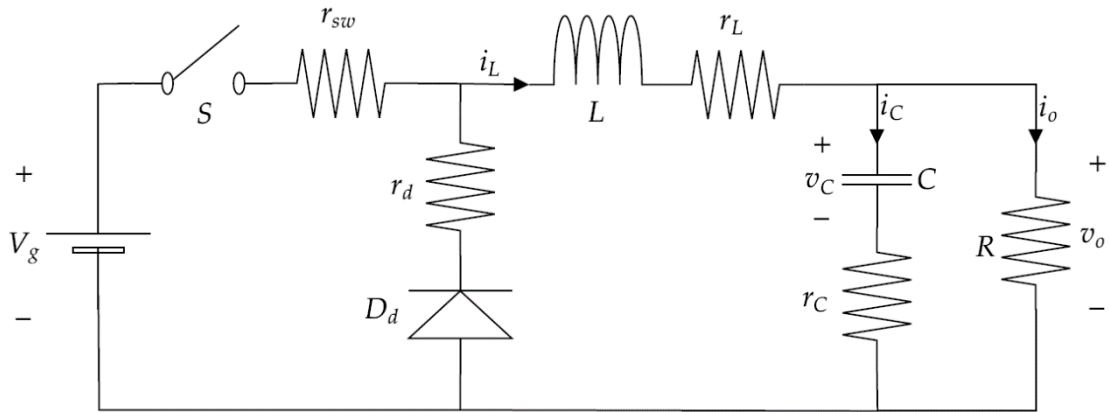


Figure 1. DC-DC buck converter circuit.

The duty-cycle-to-output-voltage transfer function of the DC-DC Buck Converter is derived from the equations formed based on the on and off states of the Switch in the CCM. The time intervals of  $0 < t < dT$  when the Switch is on, the Diode is off, and  $dT < t < T$  when the Diode is on and the Switch is off are analyzed. The variable 'd' represents the duty cycle, and 'T' denotes the Switch period (Ogata,

2010; Rashid, 2010; Erickson and Maksimović, 2020). Firstly, as seen in figure 2 when the Switch is on, and the Diode is off, the equations 1, 2 and 3 obtained for the Inductor Current, Capacitor Voltage, and Output Voltage values are as follows (Ogata, 2010; Rashid, 2010; Garg et al., 2015; Erickson and Maksimović, 2020).

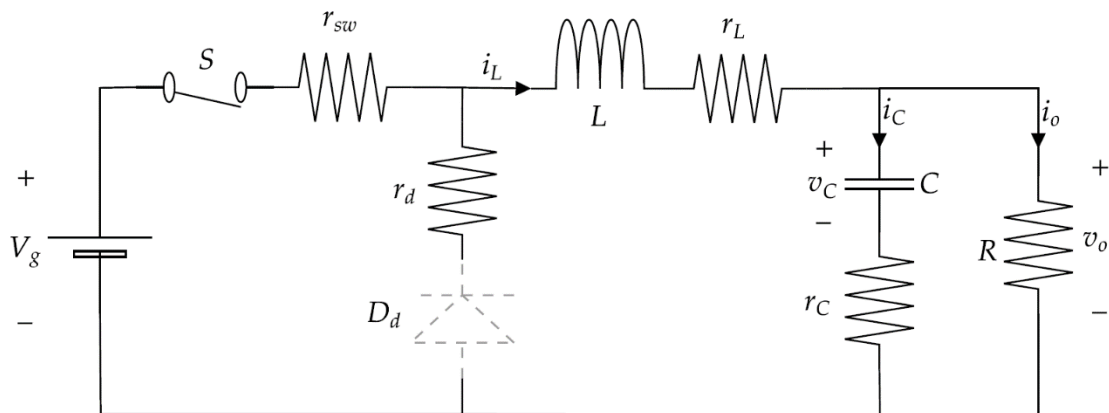


Figure 2. DC-DC buck converter circuit CCM switch on, diode off state analysis.

$$L \frac{di_L(t)}{dt} = -\left(r_{sw} + r_L + \frac{r_c R}{R + r_c}\right) i_L(t) - \frac{R}{R + r_c} v_c(t) + v_g(t) \quad (1)$$

$$C \frac{dv_c(t)}{dt} = \frac{R}{R + r_c} i_L(t) - \frac{1}{R + r_c} v_c(t) \quad (2)$$

$$v_o(t) = \frac{r_c R}{R + r_c} i_L(t) + \frac{R}{R + r_c} v_c(t) \quad (3)$$

As seen in figure 3 when the Switch is off, and the Diode is on, the equations obtained for the Inductor Current, Capacitor Voltage, and Output Voltage values are as

follows (Ogata, 2010; Rashid, 2010; Garg et al., 2015; Erickson and Maksimović, 2020).

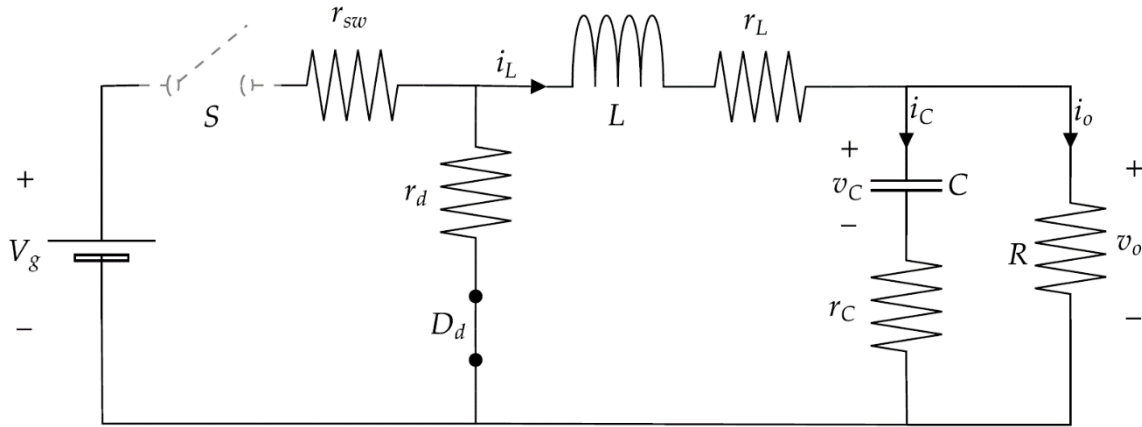


Figure 3. DC-DC buck converter circuit CCM switch off, diode on state analysis.

$$L \frac{di_L(t)}{dt} = -\left(r_d + r_L + \frac{r_c R}{R + r_c}\right) i_L(t) - \frac{R}{R + r_c} v_c(t) \quad (4)$$

$$C \frac{dv_c(t)}{dt} = \frac{R}{R + r_c} i_L(t) - \frac{1}{R + r_c} v_c(t) \quad (5)$$

$$v_o(t) = \frac{r_c R}{R + r_c} i_L(t) + \frac{R}{R + r_c} v_c(t) \quad (6)$$

The transfer function of the DC-DC Buck Converter essential for designing the PI-Lead Compensator will be derived using the State-Space Averaging (SSA) method and the equations mentioned in equations (1), 2, 3, 4, 5 and 6 mentioned earlier.

The equations in matrix form obtained during the Switch on; Diode off condition are as follows (Ogata, 2010; Rashid, 2010; Garg et al., 2015; Erickson and Maksimović, 2020). The equations in matrix form obtained during the Switch off; Diode on condition are as follows (Ogata, 2010; Rashid, 2010; Garg et al., 2015; Erickson and Maksimović, 2020).

Expanding upon the expressions in equations (7, 8, 9, 10 and 11 we obtain the following equalities (Ogata, 2010; Rashid, 2010; Garg et al., 2015; Erickson and Maksimović, 2020).

$$\dot{x}(t) = A_1 x(t) + B_1 u(t), \quad y(t) = C_1 x(t) \quad (7)$$

$$\dot{x}(t) = A_2 x(t) + B_2 u(t), \quad y(t) = C_2 x(t) \quad (8)$$

$$x(t) = \begin{bmatrix} i_L(t) \\ v_c(t) \end{bmatrix}, \quad u(t) = V_g, \quad y(t) = v_o(t) \quad (9)$$

$$A_1 = \begin{bmatrix} \frac{-1}{L} \left( r_{sw} + r_L + \frac{r_c R}{R + r_c} \right) & \frac{-R}{L(R + r_c)} \\ \frac{R}{C(R + r_c)} & \frac{-1}{C(R + r_c)} \end{bmatrix}, \quad B_1 = \begin{bmatrix} \frac{1}{L} \\ 0 \end{bmatrix}, \quad (10)$$

$$C_1 = \begin{bmatrix} \frac{r_c R}{R + r_c} & \frac{R}{R + r_c} \end{bmatrix}$$

$$A_2 = \begin{bmatrix} \frac{-1}{L} \left( r_d + r_L + \frac{r_c R}{R + r_c} \right) & \frac{-R}{L(R + r_c)} \\ \frac{R}{C(R + r_c)} & \frac{-1}{C(R + r_c)} \end{bmatrix}, \quad B_2 = \begin{bmatrix} 0 \\ 1 \end{bmatrix}, \quad C_2 = \begin{bmatrix} \frac{r_c R}{R + r_c} & \frac{R}{R + r_c} \end{bmatrix} \quad (11)$$

The formula for the transfer function that relates the BSJ Eng Sci / Kübra DOĞAN and Bülent DAĞ

duty cycle to output voltage is provided in equation (12) (Ogata, 2010; Rashid, 2010; Garg et al., 2015; Erickson and Maksimović, 2020). Equations (13) and (14) represent the steady-state values of the duty cycle ( $D$ ), the inductor current ( $I_L$ ), the output voltage ( $V_o$ ), and the input voltage ( $V_g$ ), respectively.

$$\frac{\tilde{v}_o(s)}{\tilde{d}(s)} = C(sI - A)^{-1} B_d \quad (12)$$

$$A = A_1 D + A_2 (1 - D), \quad C = C_1 D + C_2 (1 - D) \quad (13)$$

$$B_d = (A_1 - A_2) \begin{bmatrix} I_L \\ V_o \end{bmatrix} + (B_1 - B_2) V_g \quad (14)$$

Upon substituting the equations from equations (10), 11, 13 and (14) the following equalities are obtained (Ogata, 2010; Rashid, 2010; Garg et al., 2015; Erickson and Maksimović, 2020).

$$A = \begin{bmatrix} \frac{-1}{L} \left( r_x + r_L + \frac{r_c R}{R + r_c} \right) & \frac{-R}{L(R + r_c)} \\ \frac{R}{C(R + r_c)} & \frac{-1}{C(R + r_c)} \end{bmatrix}, \quad r_x = D r_{sw} + (1 - D) r_d \quad (15)$$

$$C = \begin{bmatrix} \frac{r_c R}{R + r_c} & \frac{R}{R + r_c} \end{bmatrix}, \quad B_d = \begin{bmatrix} \frac{-1}{L} ((r_d - r_{sw}) I_L + V_g) \\ 0 \end{bmatrix} \quad (16)$$

When equation (15) and (16) are substituted into equation (12), the duty cycle to output voltage transfer function is obtained as follows:

$$G_{ud}(s) = \frac{\tilde{v}_o(s)}{\tilde{d}(s)} = \frac{R((r_d - r_{sw}) I_L + V_g)(r_c C s + 1)}{(R + r_c) L C s^2 + [L + C(r_c R + (r_x + r_L)(R + r_c))] s + (R + r_x + r_L)} \quad (17)$$

## 2.2. Voltage Mode PWM Control with Pi-Lead Compensator of Dc-Dc Buck Converter

The closed-loop voltage mode PWM control diagram for the Buck Converter in the s-domain is depicted in Figur (Rashid, 2010; Erickson and Maksimović, 2020). In this diagram,  $\tilde{v}_o(s)$  represents the actual output voltage of the Buck Converter in the s-domain;  $\tilde{v}_{o,ref}(s)$  denotes the reference value for the output voltage;  $\tilde{v}_e(s)$  signifies the error value between the reference and output voltage;  $G_c(s)$  refers to the transfer function of the Compensator system;  $\tilde{v}_{con}(s)$  indicates the output of the Compensator Controller;  $G_{PWM}(s)$  corresponds to the transfer function

of the PWM modulator;  $\tilde{d}(s)$  stands for the duty value produced by the PWM;  $G_{vd}(s)$  expresses the duty-cycle-to-output-voltage transfer function of the Buck Converter circuit; and  $H(s)$  represents the feedback sensor gain (Franklin et al., 2002; Ogata, 2010; Rashid, 2010; Garg et al., 2015; Erickson and Maksimović, 2020; Nise, 2020). In voltage mode PWM control, the value obtained from the output voltage of the Buck Converter is compared to the reference voltage value, and an error signal is

generated. This error value is compensated in the  $G_c(s)$  block, producing the  $\tilde{v}_{con}(s)$  output. This output is compared to a constant sawtooth frequency curve in the PWM block, and the required switching signal for the Buck Converter switch is generated based on the obtained duty (Franklin et al., 2002; Ogata, 2010; Rashid, 2010; Garg et al., 2015; Erickson and Maksimović, 2020; Nise, 2020).

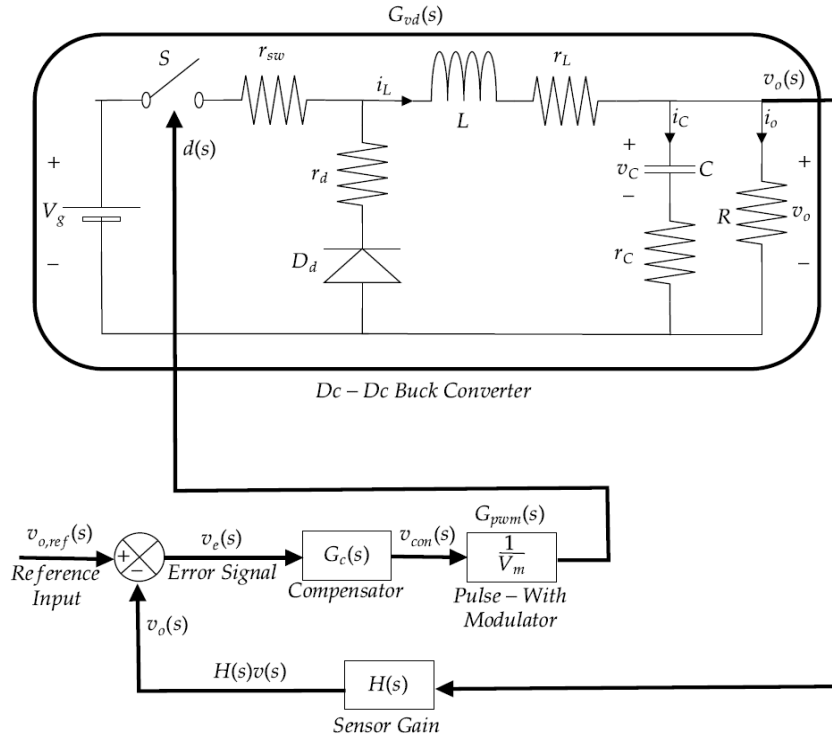


Figure 4. Closed-Loop control of DC-DC buck converter.

The open-loop transfer function of the system depicted in Figur is as follows (Ogata, 2010; Rashid, 2010; Garg et al., 2015; Erickson and Maksimović, 2020).

$$T(s) = G_c(s)G_{PWM}(s)G_{vd}(s)H(s) \quad (18)$$

In equation (18),  $G_{PWM}$  is defined as  $G_{PWM}(s) = 1/V_m$ . Here,  $V_m$  represents the peak voltage value of the sawtooth wave signal at the switching frequency. Therefore,  $T(s)$  can be expressed as follows in equation 19 (Ogata, 2010; Rashid, 2010; Garg et al., 2015; Erickson and Maksimović, 2020).

$$T(s) = G_c(s)\frac{1}{V_m}G_{vd}(s)H(s) \quad (19)$$

### 2.2.1. PI-Lead compensator design

The PI-Lead Compensator is formed by cascading the PI and Lead Compensator systems together (Pressman, 2009; Ogata, 2010; Rashid, 2010; Bishop and Dorf, 2011; Basso, 2014; Corradini, 2015; Garg et al., 2015; Erickson and Maksimović, 2020; Nise, 2020; de Azpeitia, 2021).

#### 2.2.1.1. PI compensator

Adding a PI Compensator, also known as a PI Controller, to a system allows for reducing the system's SSE and

increasing its gain in the low-frequency region (Pressman, 2009; Ogata, 2010; Rashid, 2010; Bishop and Dorf, 2011; Basso, 2014; Corradini, 2015; Garg et al., 2015; Erickson and Maksimović, 2020).

The method for the PI Compensator design involves adding a single pole to the origin. So, the PI Compensator transfer function, consisting of the  $K_p$  and  $K_i$  parameters, is as follows in equation 20 (Pressman, 2009; Ogata, 2010; Rashid, 2010; Bishop and Dorf, 2011; Basso, 2014; Corradini, 2015; Garg et al., 2015; Erickson and Maksimović, 2020; Nise, 2020; de Azpeitia, 2021).

$$G_{PI}(s) = \frac{K_p s + K_i}{s} \quad (20)$$

When deriving the closed-loop transfer function for the SSE, the following equation is obtained in equation 21 (Pressman, 2009; Ogata, 2010; Rashid, 2010; Bishop and Dorf, 2011; Basso, 2014; Corradini, 2015; Garg et al., 2015; Erickson and Maksimović, 2020; Nise, 2020; de Azpeitia, 2021).

$$\tilde{v}_e(s) = \frac{\tilde{v}_{o,ref}(s)}{1 + G_c(s)G_{PWM}(s)G_{vd}(s)H(s)} \quad (21)$$

When the PI Compensator transfer function composed of

$K_p$  and  $K_i$  parameters from equation (20) is added to  $G_c(s)$  in equation (21) the SSE is eliminated thanks to the pole at the origin (The  $1/s$  term in the denominator). While the PI Compensator is crucial in reducing steady-state errors and improving the system's response, it brings along certain disadvantages. One of the primary concerns arises from adding a pole at the origin. The presence of this pole introduces a negative shift in the system's phase, affecting its phase response. The phase response is a critical aspect of system stability. Specifically, the Phase Margin, which is the difference in phase between the system's response and -180 degrees at the GCF, is a primary indicator of the system's stability. A larger PM corresponds to more excellent stability, while a smaller PM can lead to instability. When the PI Compensator induces a negative shift in the phase, the PM of the system is reduced. A lower PM indicates a system closer to instability, which is undesirable in a control system. As such, more than relying on the PI Compensator may be required to achieve the desired system performance and stability level. Other control strategies or compensator designs need to be considered to enhance the phase margin and maintain the system's stability (Franklin et al., 2002; Ogata, 2010; Rashid, 2010; Erickson and Maksimović, 2020; Nise, 2020; de Azpeitia, 2021).

### 2.2.1.2. Lead compensator

The Lead Compensator transfer function, composed of  $K_{Lead}$ ,  $\alpha$  and  $\beta$  parameters, is given as follows in equation 22 (Pressman, 2009; Ogata, 2010; Rashid, 2010; Bishop and Dorf, 2011; Basso, 2014; Corradini, 2015; Garg et al., 2015; Erickson and Maksimović, 2020; Nise, 2020; de Azpeitia, 2021).

$$G_{Lead}(s) = \frac{K_{Lead}(s + \alpha)}{(s + \beta)}, \quad (\alpha < \beta) \quad (22)$$

The Lead Compensator is another essential control component utilized for improving system stability and response. Unlike the PI Compensator, the Lead Compensator can introduce a positive shift in the system's phase. However, it is essential to note that this positive phase shift occurs around a particular frequency known as the GCF (Ogata, 2010; Rashid, 2010; Corradini, 2015; Erickson and Maksimović, 2020).

The GCF is a critical point in the frequency domain analysis of a system. It is the frequency at which the system's open-loop gain magnitude is 1 (or 0 dB). This frequency is important because it directly relates to the system's PM, a key indicator of system stability. The PM is the difference between the phase of the system's response at the GCF and -180 degrees. A larger PM indicates a more stable system (Pressman, 2009; Ogata, 2010; Rashid, 2010; Bishop and Dorf, 2011; Basso, 2014; Corradini, 2015; Garg et al., 2015; Erickson and Maksimović, 2020; Nise, 2020; de Azpeitia, 2021).

By positively shifting the system phase at the GCF, the Lead Compensator can increase the PM, thereby enhancing system stability. However, it does not contribute to reducing the SSE (Pressman, 2009; Ogata,

2010; Rashid, 2010; Bishop and Dorf, 2011; Basso, 2014; Corradini, 2015; Garg et al., 2015; Erickson and Maksimović, 2020; Nise, 2020; de Azpeitia, 2021).

The SSE measures the system's ability to accurately track a given reference signal. A smaller SSE corresponds to better tracking performance and, therefore, better system performance. A PI Compensator is typically used to reduce the SSE and increase the system's DC Gain. However, as we have discussed, relying solely on a PI Compensator can lead to stability issues due to a decreased PM. Therefore, a combined or cascaded PI-Lead Compensator can be an appropriate choice to balance these aspects. Such a configuration aims to exploit the advantages of both compensator types. The PI Compensator's ability to reduce SSE and increase DC Gain and the Lead Compensator's capacity to enhance the PM at the desired GCF ensure overall improved system performance and stability (Pressman, 2009; Ogata, 2010; Rashid, 2010; Garg et al., 2015; Erickson and Maksimović, 2020; Nise, 2020).

### 2.2.1.3. PI-Lead compensator

When a PI-Lead Compensator is added to the system, the PI Compensator part will eliminate the SSE in the output voltage and increase the DC Gain in the low-frequency region. The Lead Compensator part will increase the PM at the desired GCF, improving the system's transient response.

The PI-Lead Compensator transfer function can be obtained as follows by multiplying the equations in equation 23 (Garg et al., 2015).

$$G_{PI-Lead}(s) = \left(\frac{K_p s + K_i}{s}\right) * \left(\frac{K_{Lead}(s + \alpha)}{(s + \beta)}\right) = \frac{K_i K_{Lead} \left(\frac{s}{K_i} + 1\right) (s + \alpha)}{s(s + \beta)}, \quad (\alpha < \beta) \quad (23)$$

If in equation 24, we denote the  $K_i * K_{Lead}$  expression as  $K$  and the  $K_i / K_{Lead}$  expression as  $\omega_z$ , the  $G_{PI-Lead}(s)$  transfer function can be expressed as follows (Garg et al., 2015).

$$G_{PI-Lead}(s) = \frac{K \left(\frac{s}{\omega_z} + 1\right) (s + \alpha)}{s(s + \beta)}, \quad (\alpha < \beta) \quad (24)$$

Step-by-step PI-Lead Compensator design for Buck converter is given below (Pressman, 2009; Ogata, 2010; Rashid, 2010; Bishop and Dorf, 2011; Basso, 2014; Corradini, 2015; Garg et al., 2015; Erickson and Maksimović, 2020; Nise, 2020; de Azpeitia, 2021).

- Step 1: In the first step, the transfer function of the uncompensated Buck Converter system is derived. As shown in equation 25, the Buck Converter can be seen as a system where the DC Gain remains consistently low in the low-frequency range. Additionally, it is characterized by having a low PM value.

$$G(s) = \frac{a_1 s + a_0}{b_2 s^2 + b_1 s + b_0} \quad (25)$$

As mentioned in earlier sections of this paper, to achieve a reduction in the SSE an increase in the DC Gain in the low-frequency region and an improvement in transient



response and overshoot values by increasing the PM at the desired GCF a PI-Lead Compensator will be designed. This compensator will consist of a PI section for SSE reduction and DC Gain enhancement and a Lead section for improving the PM at the selected GCF.

- Step 2: In the second step, a PI compensator is added to the system to increase the low-frequency gain and eliminate SSE. In equation 26, the PI Compensator equation, denoted by the corner frequency( $\omega_z$ ) is as follows:

$$G_{PI}(s) = \frac{\frac{s}{\omega_z} + 1}{s} \quad (25)$$

$\omega_z$  is placed at an appropriate frequency lower than the GCF to increase the DC gain in the low-frequency region. The transfer function of the Buck Converter system with added PI Compensator and minimized SSE effect is as follows in equation 27.

$$G_{PI-Buck}(s) = G_{PI}(s)G(s) = \left(\frac{s}{\omega_z} + 1\right) \left(\frac{a_1s + a_0}{b_2s^2 + b_1s + b_0}\right) \quad (26)$$

$$= \frac{\frac{a_1}{\omega_z}s^2 + (a_1 + \frac{a_0}{\omega_z})s + a_0}{b_2s^3 + b_1s^2 + b_0s}$$

- Step 3: In the third step, for the Buck Converter system with PI Compensator which has reduced SSE and increased low-frequency DC Gain but has a poor transient response and reduced PM value, a Lead Compensator is added to improve transient response, increased PM, and reduced overshoot. The step-by-step method for adding the Lead Compensator is as follows: The magnitude and phase values of  $G_{PI-Buck}(s)$  at the Gain Crossover Frequency ( $\omega_{gc}$ ) are determined in equation 28.

$$\varphi_{PI-Buck} = \angle G_{PI-Buck}(j\omega_{gc}), K_{PI-Buck} = |G_{PI-Buck}(j\omega_{gc})| \quad (27)$$

In order to obtain the necessary Phase Margin ( $\varphi_{Desired}$ ) and Gain Crossover Frequency values for the system, the required magnitude and phase values for the Lead Compensator are provided below in equations 29 and 30.

$$K_{req} = \frac{1}{K_{PI-Buck}} \quad (28)$$

$$\varphi_{req} = -180 - \varphi_{PI-Buck} + \varphi_{Desired} \quad (29)$$

- Step 4: If the Lead Compensator transfer function in Equation (22) is expressed in terms of magnitude, phase angle, and frequency, the resulting equations are given in Equation (30) and Equation (31) below.

$$|G_{Lead}(j\omega)| = K_{Lead} \left(\frac{\sqrt{\omega^2 + \alpha^2}}{\omega^2 + \beta^2}\right) \quad (30)$$

$$\varphi_{Lead} = \angle G_{Lead}(j\omega) = \arctan\left(\frac{\omega}{\alpha}\right) - \arctan\left(\frac{\omega}{\beta}\right) = \arctan\left(\frac{\omega * (\beta - \alpha)}{\omega^2 + \alpha\beta}\right) \quad (31)$$

As stated in equation (22), since  $\beta > \alpha$  in the Lead Compensator transfer function, the  $\varphi_{Lead}$  angle in equation (31) will always be positive.

The equation of the frequency ( $\omega_m$ ) at the maximum phase angle is as follows. To find the maximum phase

angle ( $\varphi_{Lead}$ ) and maximum magnitude ( $K_m$ ) values, substitute the formula from equation (32) for  $\omega_m$  in place of  $\omega$  in equation (31).

$$\omega_m = \sqrt{\alpha\beta} \quad (32)$$

If the maximum frequency value ( $\omega_m$ ) is expressed as the desired Gain Crossover Frequency ( $\omega_{gc}$ ), then the maximum phase angle ( $\varphi_m$ ) becomes equal to the required phase angle ( $\varphi_{req}$ ), and the maximum magnitude ( $K_m$ ) becomes equal to the required magnitude ( $K_{req}$ ).

$$\varphi_m = \frac{\omega_m(\beta - \alpha)}{\omega^2 + \alpha\beta} = \arctan\left(\frac{\beta - \alpha}{2\sqrt{\alpha\beta}}\right) \quad (33)$$

$$= \arcsin\left(\frac{\beta - \alpha}{\beta + \alpha}\right)$$

$$K_m = K_{Lead} \sqrt{\frac{\alpha}{\beta}} \quad (34)$$

To obtain the lead compensator parameters ( $K_{Lead}$ ,  $\alpha$  and  $\beta$ ), one can utilize equations (35), 37, 38, 39, 40 and 41.

$$\omega_{gc} = \omega_m = \sqrt{\alpha\beta} \quad (35)$$

$$\varphi_{req} = \varphi_m = \arcsin\left(\frac{\beta - \alpha}{\beta + \alpha}\right) \quad (36)$$

$$K_{req} = K_m = K_{Lead} \sqrt{\frac{\alpha}{\beta}} \quad (37)$$

$$K_{Lead} = K_m \sqrt{\frac{1 + \sin \varphi_{req}}{1 - \sin \varphi_{req}}} \quad (38)$$

$$\alpha = \omega_{gc} \sqrt{\frac{1 - \sin \varphi_{req}}{1 + \sin \varphi_{req}}} \quad (39)$$

$$\beta = \omega_{gc} \sqrt{\frac{1 + \sin \varphi_{req}}{1 - \sin \varphi_{req}}} \quad (40)$$

PI-Lead Compensator Design process, as can be seen from the detailed equations above, it is necessary to optimally tune the Corner Frequency ( $\omega_z$ ) in the PI Compensator Section and the Phase Margin ( $\varphi_{margin}$ ) and Gain Crossover Frequency ( $\omega_{gc}$ ) parameters in the Lead Compensator Section for the uncompensated Buck Converter system. However, no quantitative solution method or formula has been encountered in the literature for accurately adjusting these parameters. In the PI-Lead Compensator design, finding the best performance by trial and error for these three parameters at specific ranges may not be feasible. Even if possible, there would be more logical methods in terms of speed and time. Therefore, in this paper, the SA optimization algorithm, a type of artificial intelligence algorithm, has been utilized to find the most optimal values for  $\omega_z$ ,  $\varphi_{margin}$ , and  $\omega_{gc}$ . This approach enables the attainment of performance close to, if not the best, the desired values for the PI-Lead Compensator quickly and easily (Pressman, 2009; Ogata, 2010; Rashid, 2010; Bishop and Dorf, 2011; Basso, 2014; Corradini, 2015; Garg et al., 2015; Erickson and Maksimović, 2020; Nise, 2020; de Azpeitia, 2021).

**2.3. Optimally Designed PI-Lead Controller for Dc-Dc Buck Converter via Simulated Annealing Optimization Algorithm**

**2.3.1. Simulated annealing algorithm**

The Simulated Annealing Algorithm is a meta-heuristic optimization algorithm developed based on the thermal treatment of metal solids at high temperatures. SA adopts a random search method to obtain the global best solution in optimization problems where the objective function has multiple local optima (Glover and Gary, 2006; Bose, 2020; Hekimoğlu and Ekinici, 2020; Yang, 2020; Magzoub and Thamer, 2022).

Annealing is a heating process that involves gradually heating the material from high to low temperatures. In the context of metals, this technique is used to enhance their properties. The metal is heated to a high temperature, causing the internal particles to move freely and in a disordered manner. As the temperature is gradually lowered, the particles within the metal begin to stabilize and organize, resulting in a more ordered and structured state (Fraga-Gonzalez et al., 2017; Duan et al., 2018; Hekimoğlu and Ekinici, 2020; Li et al., 2022; Magzoub and Thamer, 2022).

The SA Algorithm considers a situation similar to the annealing process of metals. The process begins at a high initial temperature, and at each iteration, it generates a new candidate solution by perturbing the current solution through a random move. The algorithm evaluates the candidate solution and decides whether to accept it based on a probability distribution dependent on the current temperature and the difference in objective function values between the current and candidate solutions. The temperature parameter controls the acceptance probability of worse solutions, thus enabling the algorithm to explore the search space while avoiding local optima. The temperature is gradually and slowly reduced according to a cooling schedule (Glover and Gary, 2006; Duan et al., 2018; Hekimoğlu and Ekinici, 2020; Yang, 2020; Li et al., 2022; Magzoub and Thamer, 2022).

As the temperature parameter decreases in the SA Algorithm, it gradually converges towards stability, potentially leading to a locally optimal solution. At this stage, the algorithm has a probability of outputting the local best solution while also increasing the chance of exploring the global best solution to some extent. The algorithm's effectiveness relies on carefully selecting the initial temperature, the cooling schedule, and the particular neighborhood structure employed to generate candidate solutions (Glover and Gary, 2006; Duan et al., 2018; Hekimoğlu and Ekinici, 2020; Yang, 2020; Li et al., 2022; Magzoub and Thamer, 2022).

In the SA Algorithm, the system's state represents the solution to the optimization problem while the energy function similar to physical annealing corresponds to the function value associated with that state. The algorithm's objective is to reach the optimal solution corresponding to the state with the lowest energy level (Duan et al.,

2018; Hekimoğlu and Ekinici, 2020; Yang, 2020; Li et al., 2022; Magzoub and Thamer, 2022).

The algorithm accepts a deteriorating solution during the solution search process with a certain probability "P" and performs the annealing operation. The mentioned probability "P" formula is as follows (Simulated Annealing Options-MATLAB, 2022).

$$P = \begin{cases} 1, & dy < 0 \\ \frac{1}{1 + \exp\left(\frac{dy}{T}\right)}, & dy \geq 0 \end{cases} \quad (41)$$

In Equation 42, dy represents the difference in cost function between the new solution and the current solution ( $dy = y(x2) - y(x1)$ ). If  $dy < 0$ , the probability of accepting the new solution P is 1. Otherwise, if  $dy \geq 0$ , the probability of accepting the new solution is given by

$$\frac{1}{1 + \exp\left(\frac{dy}{T}\right)}$$

In equation (41), T represents the annealing temperature, which varies depending on the initial annealing temperature,  $T_0$ . The relationship between them is as follows (Duan et al., 2018).

$$T_{k+1} = \alpha T_k \quad (42)$$

In equation (42), the parameter  $\alpha$  is generally considered to be between 0.8 and 1. This paper considers the  $\alpha$  value 0.95 (the default value). In this way, during the initial cooling stages, the temperature remains relatively high, allowing the possibility of escaping from the optimal solution (Fraga-Gonzalez et al., 2017; Duan et al., 2018; Simulated Annealing Options-MATLAB, 2022).

In this paper, the parameters of the SA Algorithm utilized for the optimization process of the PI-Lead Compensator parameters designed for the Buck Converter are presented in table 1 (Magzoub and Thamer, 2022). The variable n represents the number of variables for which the Simulated Annealing will find the optimum. In this paper, the value of n has been set to 3. These variables are for the PI-Lead Compensator to be designed for the Uncompensated Dc-Dc Buck Converter System: the corner frequency ( $\omega_z$ ) the bandwidth also known as Gain Crossover Frequency (GCF or  $\omega_{gc}$ ), and the Phase Margin parameters.

**Table 1.** Parameters of the simulated annealing algorithm

Parameter	Value
Max Iterations	Inf
Time Limit	Inf
Objective Limit	Inf
Annealing Function	Fast Annealing
Max Function Evaluations (3000 x n)	9000
Function Tolerance	$1 \times 10^{-6}$
Max Stall Iterations (500 x n)	1500
Reannealing Interval	100

**2.3.2. PI-Lead controller optimization via simulated annealing**

The open-source project, referenced as (Buck-Converter-PI-Lead-Compensator-SA, 2022), featuring performance analysis and identification of optimal PI-Lead Compensator parameters for DC-DC Buck Converters via the SA Algorithm, was developed using MATLAB within the scope of this paper.

The DC-DC Buck Converter circuit parameters, considered for conducting performance analysis and designing an appropriate PI-Lead Compensator, are provided in table 2.

**Table 2.** Parameters of Dc-Dc buck converter circuit

Parameter	Value
Input Voltage ( $V_{in}$ )	60 V
Output Voltage ( $V_{out}$ )	48 V
Output Power ( $P_{out}$ )	2400 W
Inductance	6.2 $\mu$ H
Capacitance	45 $\mu$ F
Load Transient Response ( $\leq$ % of $V_{out}$ )	10
Inductance Current Ripple ( $D_{iL}$ )	20
Switch Frequency ( $f_{sw}$ )	200 kHz
Switch-on resistance ( $r_{sw}$ )	14 m $\Omega$
Diode forward resistance ( $r_d$ )	1 m $\Omega$
Inductance ESR ( $r_L$ )	1.3 m $\Omega$
Capacitance ESR ( $r_C$ )	1.72 m $\Omega$
Sawtooth Peak ( $V_m$ )	1
Sensor Gain ( $H(s)$ )	1

In figure 4 the open-loop transfer function formula for the uncompensated DC-DC Buck Converter System is as follows.

$$T_{uncomp}(s) = \frac{1}{V_m} G_{vd}(s)H(s), \quad V_m = 1, \quad (43)$$

$$H(s) = 1 \text{ (from table 2)}$$

$$r_x = Dr_{sw} + (1 - D)r_d \text{ (from equation 15)} \quad (44)$$

In Table, when the parameters are substituted into the equation for the open-loop transfer function of the DC-DC Buck Converter given in equations (43) and (44), the uncompensated system transfer function is obtained and presented in equation (45).

$$G_{vd}(s) = \frac{1.644 * 10^4 s + 2.123 * 10^{11}}{s^2 + 2.543 * 10^4 s + 3.625 * 10^9} \quad (45)$$

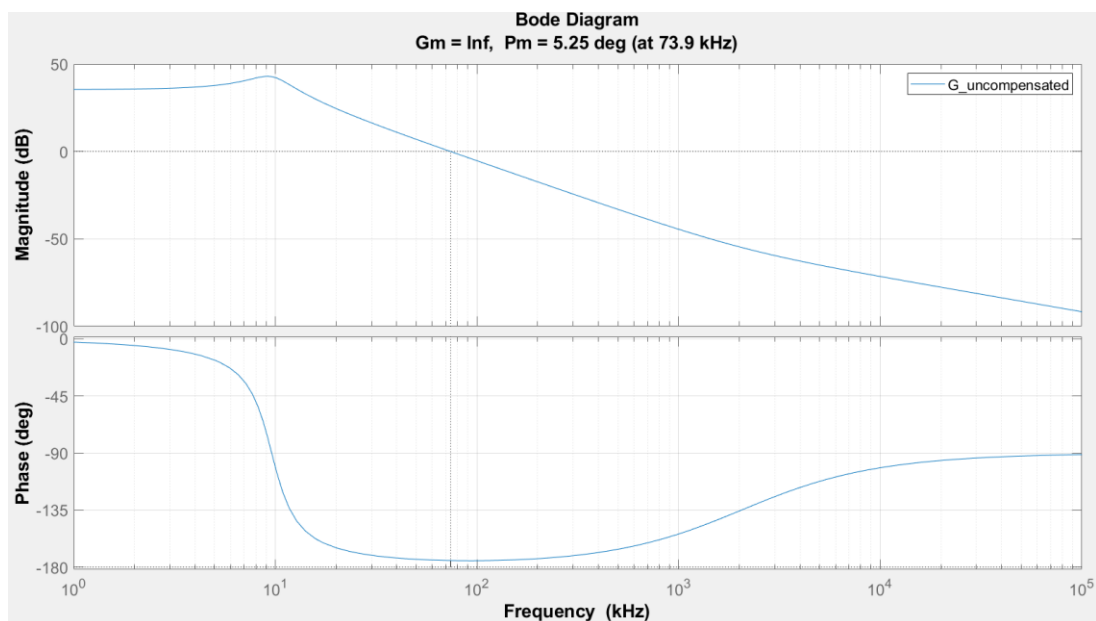


**Figure 5.** Frequency response of uncompensated DC–DC buck converter.

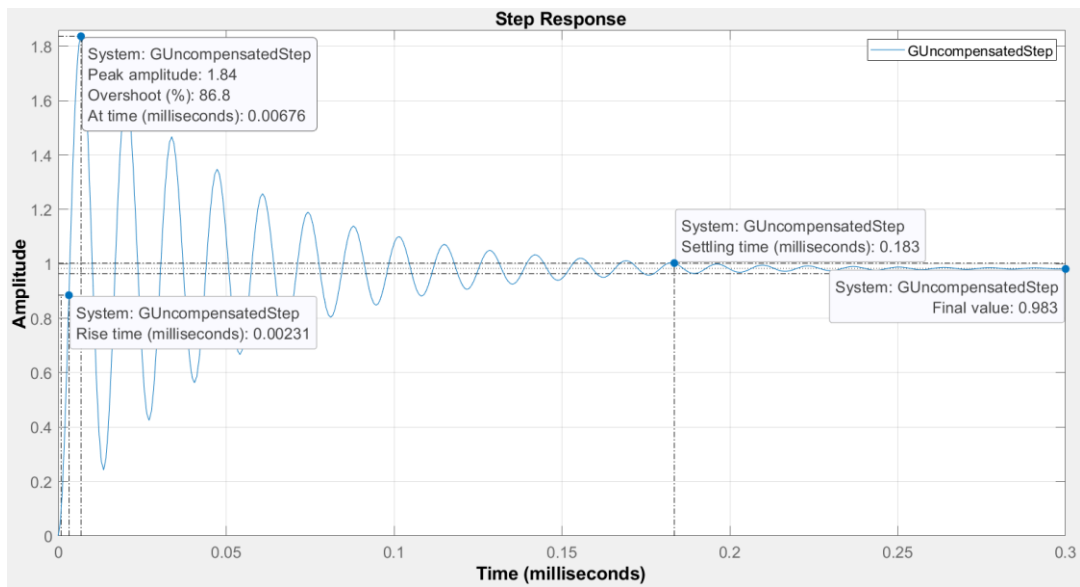


Figure 6. Step response of uncompensated DC-DC buck converter.

The frequency response (Bode plot) of the transfer function in Equation (45) is shown in Fig, while the step response is depicted in Fig.

If the frequency response and step response curves of the Uncompensated DC-DC Buck Converter System, which are located in Fig and Fig, are to be evaluated;

- PM is 5.25°, and the Overshoot (86.8%) and oscillation observed in the Step response curve in figure 6 are excessive. The transient response (settling time) value needs to be faster than 0.000183. In other words, the system response is slow. The system needs to be accelerated. For better transient response, the PM value should be at least 45° (Pressman, 2009; Ogata, 2010; Bishop and Dorf, 2011; Garg et al., 2015).
- As seen in figure 5, the Bandwidth, also known as GCF, is 73.9 kHz. The GCF value should be between Switch Frequency( $f_{sw}$ )/4 and Switch Frequency( $f_{sw}$ )/10 (i.e., according to the Switch Frequency value in table 2, it

should be between 50 kHz and 20 kHz) (Pressman, 2009; Ogata, 2010; Bishop and Dorf, 2011; Garg et al., 2015).

- The gain value in the low-frequency region is constant and low. Therefore, as shown in figure 6, the SSE could not be eliminated. For the SSE value to be reduced or eliminated in the range between 100Hz and 1kHz, the slope of the gain in the low-frequency region should preferably be -20 dB/decade (Pressman, 2009; Ogata, 2010; Bishop and Dorf, 2011; Garg et al., 2015). The block diagram for the DC-DC Buck Converter System, which includes a PI-Lead Compensator controller, can be seen in figure 7, as listed in table 2. The block diagram depicting the PI-Lead Compensator controller for the DC-DC Buck Converter System can be observed in figure 7. The DC-DC Buck Converter block within this diagram represents the transformed values of table 2 in the s-domain.

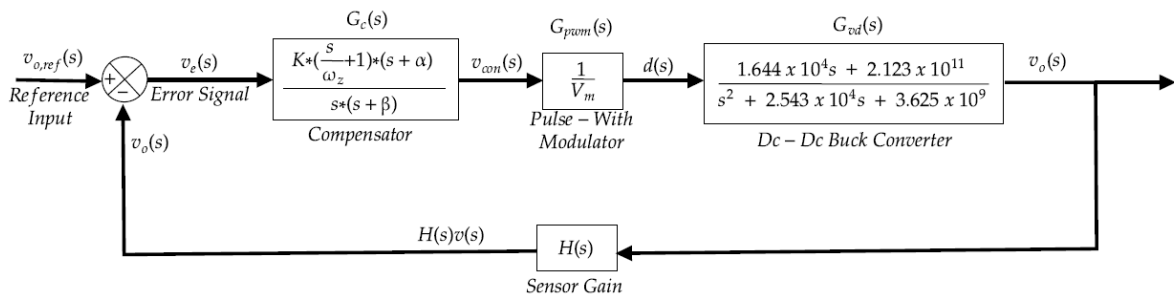


Figure 7. Buck converter system with PI-Lead compensator.

The SA optimization algorithm was utilized to determine the most optimal values for the parameters Corner Frequency ( $\omega_z$ ), bandwidth, also known as GCF ( $\omega_{gc}$ ), and PM for a PI-Lead Compensator that will be designed for the Uncompensated DC-DC Buck Converter (Pressman, 2009; Ogata, 2010; Rashid, 2010; Bishop and Dorf, 2011; Basso, 2014; Corradini, 2015; Garg et al., 2015; Erickson

and Maksimović, 2020; Nise, 2020; de Azpeitia, 2021). The detailed conceptual flow chart of the Simulated Annealing optimization approach is depicted in figure 8. The equation for the objective function ( $J$ ), also known as the cost function, created for the error function represented in the flow chart in figure 8, is found by the equation below.

$$J(\text{CostFunction}) = (1 - e^{-\alpha})(E_{ss} + E_{\text{Overshoot}} + E_{\text{Undershoot}}) + e^{-\alpha}(T_s + T_r) \quad (46)$$

In the equation represented by Equation (46), the following terms are defined (Ogata, 2010; Rashid, 2010; Bishop and Dorf, 2011; Basso, 2014; Garg et al., 2015; Erickson and Maksimović, 2020; Hekimoğlu and Ekinci, 2020).

- $E_{ss}$  = SSE (Steady State Error),
- $E_{\text{Overshoot}}$  = Percentage Overshoot,
- $E_{\text{Undershoot}}$  = Percentage Undershoot,
- $T_s$  = Settling Time (Transient Response),
- $T_r$  = Rise Time (Rise Time),
- $\alpha$  represents the coefficient factor.

In this paper, the maximum number of iterations, as

indicated in the flow chart in

Figure 8 has been taken as 5. Consequently, the outputs of each iteration in the optimization process of the PI-Lead compensator parameters, which will be added to the Buck Converter system presented in table 2, using Simulated Annealing, are provided in table 3. According to these outputs, the bode diagrams and step response graphs, obtained in both the frequency and time domain, are presented in figure 9 and 10.

In order to minimize the possibility of getting trapped in local minima, the Simulated Annealing algorithm is run multiple times from randomly chosen points. The Number of Restarts parameter defines the number of these reruns. The Number of Restarts is set to 5 for this study, and table 3 is generated.

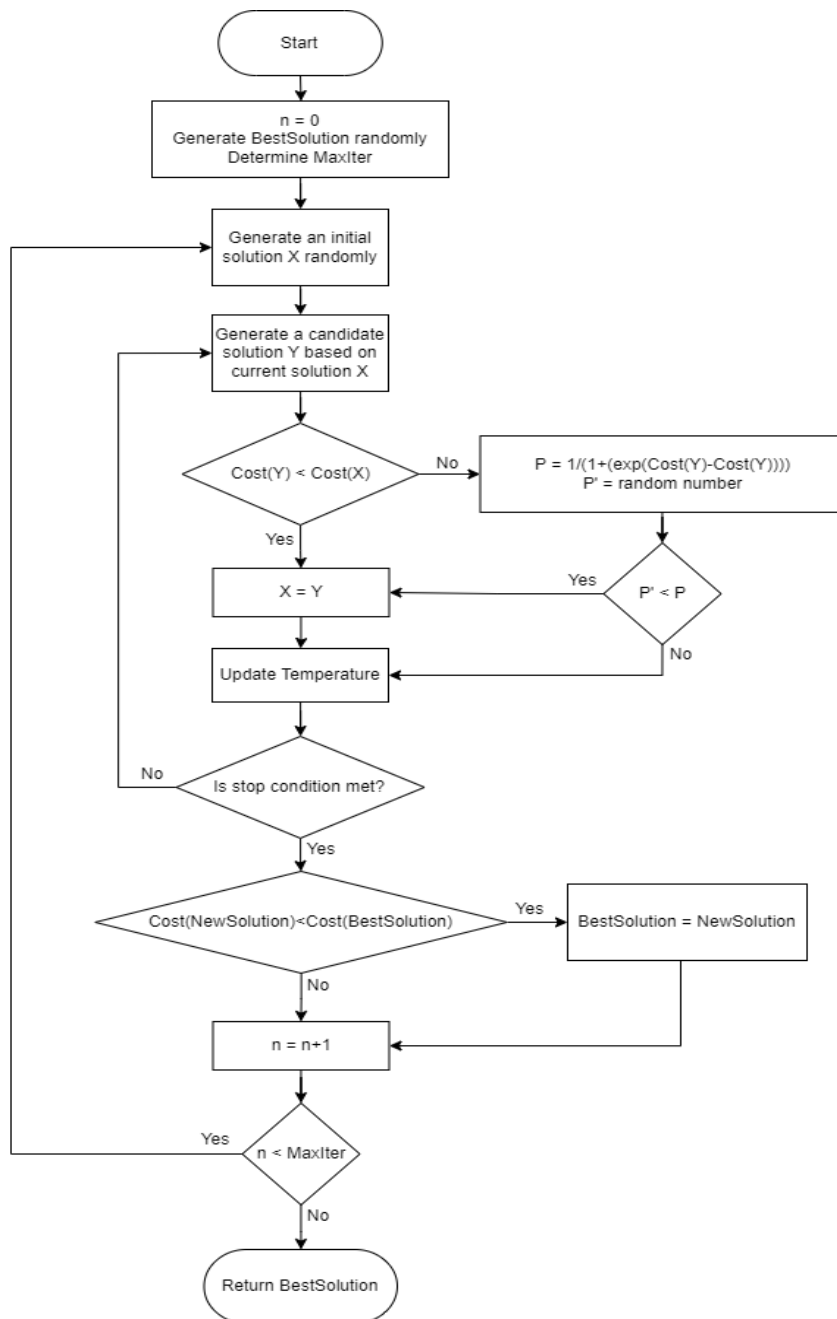
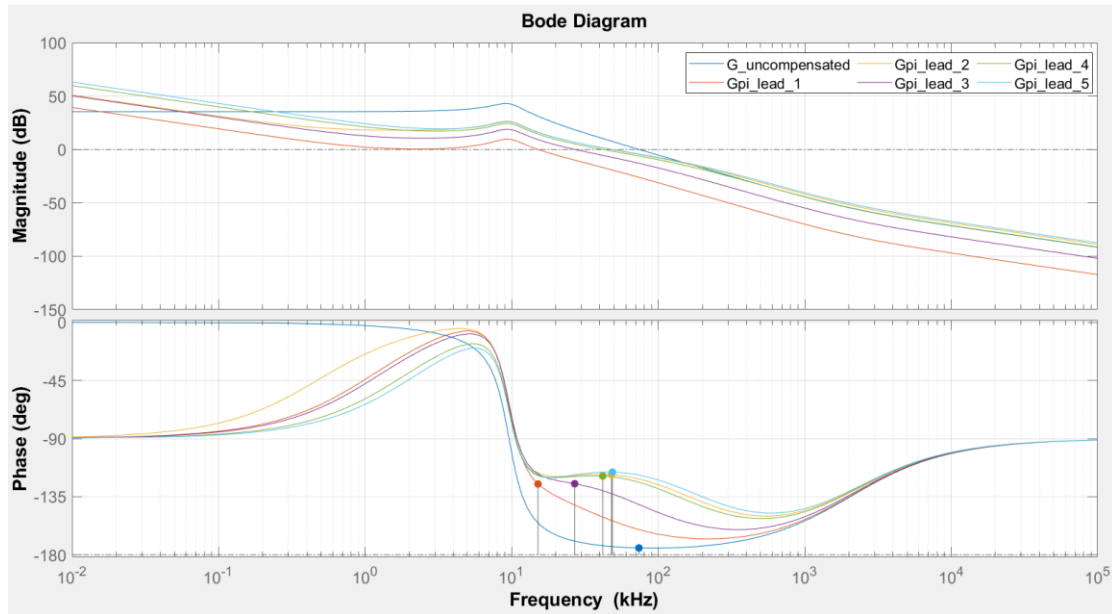


Figure 8. Flow chart of the simulated annealing optimization approach.



**Table 3.** Dc-Dc Buck converter system Pi-Lead compensator parameters: Outputs of Sa algorithm iterations

Number of Restart	Output of Cost Function	Corner Frequency (Hz)	Crossover Frequency (Hz)	Phase Margin
1	173.0030	1064	15174	55
2	0.1774	478	48172	62
3	0.2618	1172	26937	55
4	0.1243	1789	41900	61
5	0.0955	2153	48787	64



**Figure 9.** Compensated DC-DC buck converter with SA optimization frequency domain outputs.

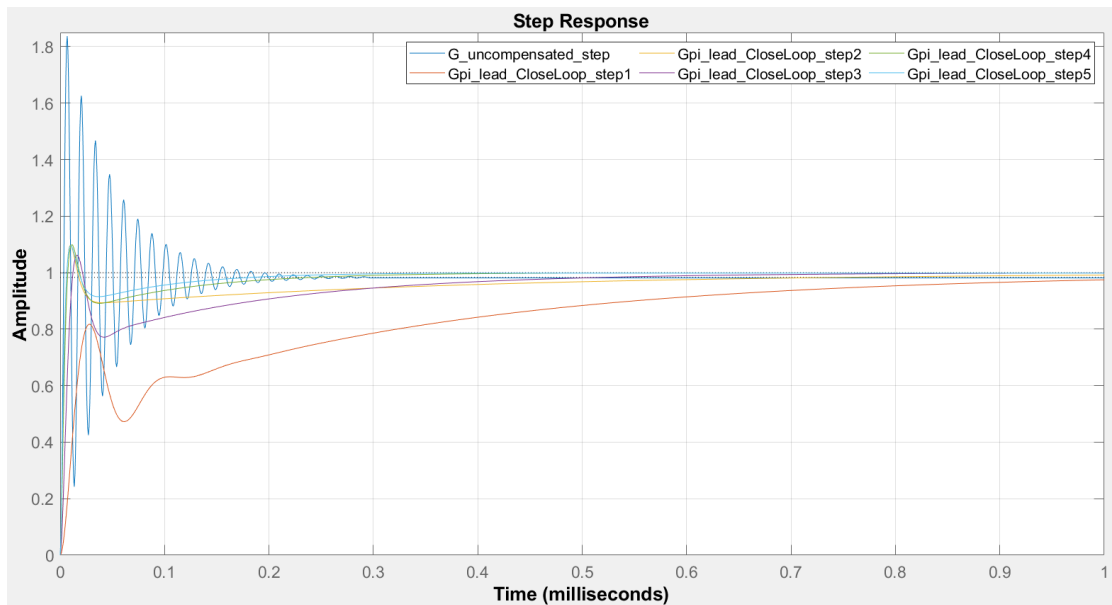


**Figure 10.** Compensated DC-DC buck converter with SA optimization time domain output.

### 3. Results and Discussion

As seen in table 4, the probability of approaching the optimal values for each parameter increases as the number of iterations increases. Each step generates the SA outcome in this procedure by starting from an independently random point. Since steps are executed

independently, it cannot be guaranteed that the results will improve at every step. When computing the best solution, the value with the lowest cost among all steps is considered the optimal solution. This operation aims to minimize the probability of encountering poor results due to the risk of SA getting trapped in local minima.

Therefore, the larger the maximum number of iterations, the higher the probability of identifying the global optimum value as the best solution.

In this paper, the transfer function from the duty cycle to the output voltage of a non-ideal DC-DC Buck Converter has been derived using the state-space averaging technique. Subsequently, a PI-Lead Compensator controller has been utilized for voltage mode PWM control, regulating the DC-DC output voltage. The parameters of this cascaded structure have been optimized using the Simulated Annealing algorithm, resulting in the improvement of the DC-DC Buck Converter system's Phase Margin, Gain Crossover Frequency (GCF), and low-frequency gain parameters, thereby enhancing its output performance.

The use of the Simulated Annealing algorithm has expedited the determination of PI-Lead Compensator parameters. This algorithm efficiently provides the most suitable value within the specified lower and upper limits, eliminating trial and error and minimizing the possibility of prediction errors. Furthermore, through multiple simulated iterations, the SA algorithm has demonstrated its effectiveness in finding optimal solutions in complex and broad search spaces for optimizing PI-Lead Compensator parameters. An essential advantage of this process is the adjustability of the iteration count, allowing fine-tuning for optimal results. As a result, the challenges encountered in controller design have been significantly reduced.

**Table 4.** Dc-Dc Buck Converter System Pi-Lead Compensator Outputs of Sa Algorithm Iterations

Number of Restart	Output of Cost Function	Overshoot (%)	Rise Time (s)	Settling Time (Transient Response) (s)	Steady State Error	Low Frequency Region Gain (dB)
-	Uncomp	86.8	2.31e-06	183e-06	0.983	35.4 (Constant)
1	173,0030	< 1(Unstable)	545e-06	1080e-06	1	20 (Slope)
2	0,1774	9.69	4.37e-06	680e-06	1	19.6 (Slope)
3	0,2618	6.2	8.22e-06	488e-06	1	19.8 (Slope)
4	0,1243	9.88	4.99e-06	222e-06	1	19.9 (Slope)
5	0,0955	9.55	4.35e-06	168e-06	1	20 (Slope)

However, it is essential to note that the Simulated Annealing algorithm may encounter the possibility of getting trapped in local minima. As a result, the probability of finding the global minimum value with the Simulated Annealing algorithm is maximized by starting from random points for a few iterations, as determined by the maximum iteration count. Therefore, the algorithm's efficiency is subject to its implementation and parameter settings.

The results obtained in this study provide evidence that optimizing controller parameters significantly improves the performance of the Buck Converter. Moreover, this optimization method is not limited to determining PI-Lead Compensator parameters designed explicitly for the DC-DC Buck Converter; it can also be adapted for optimizing parameters of similar compensator systems designed for other types of DC-DC converters.

This study demonstrates the potential for using heuristic algorithms in electronic circuit design for broader applications. As future work, it may be suggested to investigate the efficacy of other heuristic algorithms (for example, Genetic Algorithm, Particle Swarm Optimization, etc.) in the design of the PI-Lead compensator controller.

**Author Contributions**

The percentage of the author(s) contributions is presented below. All authors reviewed and approved the final version of the manuscript.

	K.D.	B.D.
C	50	50
D	50	50
S	50	50
DCP	50	50
DAI	50	50
L	50	50
W	50	50
CR	50	50
SR	50	50
PM	50	50
FA	50	50

C=Concept, D= design, S= supervision, DCP= data collection and/or processing, DAI= data analysis and/or interpretation, L= literature search, W= writing, CR= critical review, SR= submission and revision, PM= project management, FA= funding acquisition.

**Conflict of Interest**

The authors declared that there is no conflict of interest.

**Ethical Consideration**

Ethics committee approval was not required for this study because of there was no study on animals or humans.

### Acknowledgements

This study has emerged as a part of my master's thesis, and I would like to express my deep gratitude to my advisor for his unwavering support throughout this process. I would like to thank ASELSAN A.Ş., who financed a part of my research and furthered my research by providing technical information and approval. Kübra DOĞAN, as the author, expresses her gratitude to this valuable institution for her contributions at every stage of the collection of outputs, data analysis and article writing. I would like to thank all the people and institutions who contributed, especially ASELSAN, for making this research happen.

### References

- Amaral AMR, António JMC. 2022a. Simulation tool to evaluate fault diagnosis techniques for DC-DC converters. *Symmetry* 14(9): 1886. DOI: 10.3390/sym14091886.
- Amaral AMR, António JMC. 2022b. Using python for the simulation of closed-loop pi controller for a buck converter. *Signals*, 3(2): 313-325. DOI: 10.3390/signals3020020.
- Basso CP. 2014. *Switch-Mode power supplies*. McGraw Hill, New York, USA, 2<sup>nd</sup> ed., pp: 117.
- Bishop RC, Dorf RH. 2011. *Modern control systems*. Pearson, New York, USA, pp: 1104.
- Bose BK. 2002. *Modern power electronics & AC drives*. Prentice Hall, London, UK, pp: 736.
- Bose BK. 2020. *Power electronics and motor drives: advances and trends*. Academic Press, London, UK, pp: 934.
- Buck-Converter-PI-Lead-Compensator-SA. 2022. URL: <https://github.com/kd94/Buck-Converter-PI-Lead-Compensator-SA> (Accessed date: March, 15, 2022).
- Chibante R. 2010. *Simulated annealing: theory with applications*. Intechopen, London, UK, pp: 302.
- Corradini L. 2015. *Digital control of high-frequency switched-mode power converters*. John Wiley & Sons-IEEE Press, London, UK, pp: 368.
- de Azpeitia MAP. 2021. *Design and control of power converters 2019*. MDPI, Basel, Switzerland, pp: 402.
- Duan W, Zhang H, Wang C. 2018. Deformation estimation for time series InSAR using simulated annealing algorithm. *Sensors*, 19(1): 115. DOI: 10.3390/s19010115.
- Eiben AE, James ES. 2015. *Introduction to evolutionary computing*. Springer-Verlag, Berlin, Heidelberg, Germany, pp: 287.
- Ekinci S, Baran H. 2019. Improved kidney-inspired algorithm approach for tuning of PID controller in AVR system. *IEEE Access*, 7: 39935-39947. DOI: 10.1109/ACCESS.2019.2906980.
- Erickson RW, Maksimović D. 2020. *Fundamentals of power electronic*. Springer, Cham, New York, USA, 3<sup>rd</sup> ed., pp: 1103.
- Feng T, Yu D, Wu B, Wang H. 2023. A micro-hotplate-based oven-controlled system used to improve the frequency stability of mems resonators. *Micromachines*, 14(6): 1222. DOI: 10.3390/mi14061222.
- Fraga-Gonzalez LF, Fuentes-Aguilar RQ, Garcia-Gonzalez A, Sanchez-Ante G. 2017. Adaptive simulated annealing for tuning PID controllers. *AI Commun*, 30(5): 347-362. DOI: 10.3233/AIC-170741.
- Franklin GF. 2002. *Feedback control of dynamic systems*. Upper Saddle River: Prentice hall, London, UK, pp: 928.
- Gaing Z-L. 2004. A Particle swarm optimization approach for optimum design of PID controller in AVR system. *IEEE*, 19(2): 384-391. DOI: 10.1109/TEC.2003.821821.
- Garg, Man M, Yogesh VH, Mukesh KP. 2015. Design and performance analysis of a Pwm Dc–Dc buck converter using PI-Lead compensator. *Arab J Sci Engin*, 40: 3607-3626. DOI: 10.1007/s13369-015-1838-z.
- Glover FW, Gary AK. 2006. *Handbook of metaheuristics*. Springer Science & Business Media, London, UK, pp: 570.
- Hekimoğlu B, Serdar E. 2020. Optimally designed PID controller for a DC-DC buck converter via a hybrid whale optimization algorithm with simulated annealing. *Electrica*, 20(1): 19-27. DOI: 10.5152/electrica.2020.19034.
- Kazimierczuk MK. 2015. *Pulse-width modulated DC-DC power converters*. John Wiley & Sons, London, UK, pp: 960.
- Li H, Hui YB, Wang Q, Wang HX, Wang LJ. 2022. Design of anti-swing pid controller for bridge crane based on PSO and SA algorithm. *Electronics*, 11.19: 3143. DOI: 10.3390/electronics11193143.
- Magzoub MA, Thamer A. 2022. Optimal design of automatic generation control based on simulated annealing in interconnected two-area power system using hybrid PID—fuzzy control. *Energies*, 15.4: 1540. DOI: 10.3390/en15041540.
- Middlebrook RD, Slobodan C. 1976. A general unified approach to modelling switching-converter power stages. *IEEE Power Electronics Specialists Conference*, June 8-10, Cleveland, OH, USA, pp: 18-34. DOI: 10.1080/00207217708900678.
- Mohan N, Tore M. 2003. *Power electronics: converters, applications, and design*. John Wiley & Sons, London, UK, pp: 832.
- Moorthi VR. 2005. *Power electronics: devices, circuits and industrial applications*. Oxford University Press, London, UK, pp: 1028.
- Nalepa R, Karol N, Błażej S. 2020. Hybrid tuning of a boost converter pi voltage compensator by means of the genetic algorithm and the d-decomposition. *Energies*, 14.1: 173. DOI: 10.3390/en14010173.
- Nise NS. 2020. *Control systems engineering*. John Wiley & Sons, London, UK, pp: 800.
- Ogata K. 2010. *Modern control engineering*. Upper Saddle River, Prentice Hal, New Jersey, USA, pp: 904.
- Pressman AI. 2009. *Switching power supply design*. McGraw-Hill Education, New York, USA, pp: 550.
- Qu J, Zhang Z, Li H, Li M, Xi X. 2023. Design and experiments of a two-stage fuzzy controller for the off-center steer-by-wire system of an agricultural mobile robot. *Machines*, 11.2: 314. DOI: 10.3390/machines11020314.
- Rashid MH. 2010. *Power electronics: circuits, devices, and applications*. Pearson, New York, USA, pp: 1031.
- Rashid MH. 2017. *Power electronics handbook*. Butterworth-Heinemann, Berlin Germany, pp: 254.
- Simulated Annealing Options-MATLAB. 2022. URL: <https://www.mathworks.com/help/gads/simulated-annealing-options.html#bq26j8s-4> (Accessed date: March, 15, 2022).
- Suntio T, Messo T. 2019. *Power electronics in renewable energy systems*. MDPI AG, Basel, Switzerland, pp:604.
- Surya S, Mohan KS, Sheldon W. 2021. Modeling of average current in non-ideal buck and synchronous buck converters for low power application. *Electronics*, 10(21): 2672. DOI: 10.3390/electronics10212672.
- Surya S, Sheldon W. 2021. Generalized circuit averaging technique for two-switch PWM DC-DC converters in CCM. *Electronics*, 10(4): 392. DOI: 10.3390/electronics10040392.
- Surya S, Sheldon W. 2021. Modeling of average current in ideal and non-ideal boost and synchronous boost converters.

- Energies, 14(16): 5158. DOI: 10.3390/en14165158.
- Umanand L. 2009. Power Electronics: essentials \& applications. Wiley India Pvt. Limited, London, UK, pp: 944.
- Volkov T. 2015. Fundamentals of power electronics. Scitus Academics LLC, London, UK, pp: 306.
- Wang X, Bingwen Q, Hongdong W. 2021. Comparisons of Modeling Methods for Fractional-Order Cuk Converter. Electronics, 10.06: 710. DOI: 10.3390/electronics10060710.
- Yang C, Xie F, Chen Y, Xiao W, Zhang B. 2020. Modeling and analysis of the fractional-order flyback converter in continuous conduction mode by caputo fractional calculus. Electronics, 9(9): 1544. DOI: 10.3390/electronics9091544.
- Yang XS. 2020. Nature-inspired optimization algorithms. Academic Press, London, UK, pp: 160.
- Zeb K, Nazir MS, Ahmad I, Uddin W. 2021. Control of transformerless inverter-based two-stage grid-connected photovoltaic system using adaptive-pi and adaptive sliding mode controllers. Energies, 14(9): 2546. DOI: 10.3390/en14092546.